

130 GeV Gamma Ray Signal in NMSSM by Internal Bremsstrahlung

Gaurav Tomar,^{*} Subhendra Mohanty,[†] and Soumya Rao[‡]

Physical Research Laboratory, Ahmedabad 380009, India

Abstract

There is a possible γ -ray signal at 130 GeV coming from the Galactic Center as seen by Fermi-LAT experiment. We give a SUSY dark matter model to explain this γ -ray feature in NMSSM. We show that in NMSSM, one can have a benchmark set in which the γ -ray signal arises from final state γ 's in the $\chi\chi \rightarrow f\bar{f}\gamma$ annihilation of a 130 GeV bino dark matter requiring a boost factor of ~ 590 to fit the γ -ray signal. In addition, this benchmark set also gives the correct relic density, lightest Higgs mass of 125 GeV and is consistent with constraints on SUSY from LHC. This dark matter model evades the XENON100 constraint but is testable in a future XENON1T experiment.

^{*} tomar@prl.res.in

[†] mohanty@prl.res.in

[‡] soumya@prl.res.in

I. INTRODUCTION

The minimal supersymmetric standard model (MSSM)[1] is an extension of the standard model, in which the Higgs mass is protected from receiving large radiative corrections and in addition it has a plethora of weakly interacting neutral particles, which can serve as candidates for dark matter. MSSM has the problem of explaining the scale of the μ parameter, which is addressed by extending MSSM with an additional gauge singlet superfield in the so called NMSSM (Next-to-Minimal Supersymmetric Standard Model) [2–9], where the μ parameter can arise from the vev of the singlet field.

The Higgs sector of NMSSM contains three CP-even mass eigenstates, the lowest of which is interpreted as the 125 GeV Higgs, discovered at LHC [10, 11]. In NMSSM, Higgs mass gets an additional contribution from the singlet-Higgs interaction in the scalar potential, which helps to achieve 125 GeV Higgs mass after loop corrections.

The neutral sector of NMSSM has five mass eigenstates, four gauginos from MSSM and in addition a singlino component. In NMSSM, there are two extra candidates for dark matter compared to MSSM, namely the scalar singlet and its superpartner singlino. A viable dark matter must satisfy the relic density $\Omega_\chi h^2 = 0.1199 \pm 0.0027$, observed by WMAP-PLANCK [12, 13] and it should also satisfy the bounds from direct detection experiments like XENON100, CDMS [14–16] etc. There are hints of possible signals of dark matter in cosmic ray and like the 130 GeV gamma ray signal from the Galactic Center, observed by Fermi-LAT experiment [17], which can be explained by the dark matter of mass ~ 130 GeV and annihilation cross-section $\langle\sigma v\rangle_{\gamma\gamma} = 1.27 \pm 10^{-27} \text{cm}^3 \text{sec}^{-1}$ [18–26]. There are also present some non dark matter explanations of the 130 GeV gamma ray signal, like instrumental noise [27], statistical fluctuation, Earth-limb magnification [28] and emission from AGNs [25], but in our work, we focused on the dark matter explanation of this signal.

To satisfy Fermi-LAT data [17], we require large dark matter annihilation cross-section with $m_\chi \sim 130$ GeV [18]. Within MSSM, if one requires a large annihilation cross-section into photons, it could mean that neutralino dark matter is a higgsino, wino or mixture of them. However if dark matter is a 130 GeV higgsino or wino, then the annihilation cross-section at freeze out will be large and that would lead to a negligible thermal relic density. In addition a wino or higgsino annihilation would give a continuum gamma ray spectrum [29], which constraints these models. In [30], a bino dark matter of 130 GeV produces gamma

rays through the internal bremsstrahlung ($\chi\chi \rightarrow f\bar{f}\gamma$), which makes use of well known fact [31, 32] that if we add a photon in $\chi\chi \rightarrow f\bar{f}$ annihilation then we can get rid from helicity suppression factor $(m_f/m_\chi)^2$, but of course paying the price of α_{em} suppression. As it has been pointed out [30], if we want a lightest supersymmetric particle (LSP) in the form of pure bino then we would need to make the higgsinos fraction small by taking a large value of $\mu \gtrsim 500$ GeV. This leads to the naturalness issue in MSSM, where the μ parameter is expected to be 100 – 200 GeV. A way out is in NMSSM, where an extra contribution comes to the higgsinos masses from singlino-higgsinos mixing. Making this mixing large ensures that higgsinos are heavy and their contribution in LSP become small, keeping this model natural. In NMSSM, one can also raise dark matter annihilation cross-section through a resonance channel, for which the mass of pseudo scalar tuned as $m_A \approx 2m_{\chi^0}$ [33, 34]. This involves tuning in parameters of two unrelated sector of the model, which does not seem natural. So, internal bremsstrahlung in NMSSM provides a more natural way to explain the observed feature of Fermi-LAT.

In this paper, we studied NMSSM and present a set of bench mark point, in which LSP is a bino with mass ~ 130 GeV. The correct relic density has been obtained by taking low stau mass and it is achieved by stau-coannihilation. In the Higgs sector, one can have 125 GeV higgs by taking $\hat{H}_u \cdot \hat{H}_d \hat{S}$ coupling $\lambda \sim -0.62$, the same large lambda in the neutralino sector ensures that the higgsino are heavy due to singlino-higgsino mixing and the μ parameter need not to be tuned for the large value of higgsinos components. The gamma ray signal comes by internal bremsstrahlung ($\chi\chi \rightarrow f\bar{f}\gamma$) and therefore we need not tune the pseudo scalar mass to twice the bino mass as in the other NMSSM models [33, 34], which explain the 130 GeV signal.

We used micrOMEGAs code 3.1 [35] and computed the gamma-ray flux, electron-positron flux and antiproton flux from the annihilation of 130 GeV bino dark matter. We used these fluxes in GALPROP code [36, 37], following isothermal dark matter density profile [38] and found that assuming a boost factor [39, 40] of ~ 590 , we can explain the 130 GeV gamma-ray signal, while still not exceeding the electron, positron and antiproton data [41–44]. We also find that our bench mark values of parameters ensure small direct detection cross-section, such that there is no signal for this dark matter in XENON100 experiment [14] but we predict a scattering cross-section of $O \sim 10^{-46} \text{cm}^2$, which may be seen in XENON1T experiment [45].

The arrangement of the paper is as follows. In section II, we discussed the general NMSSM model and compared the output of our model with their Standard Model counterparts. In section III, we discussed internal bremsstrahlung in detail. After describing the perspective of our bench mark point for the direct and indirect detection of dark matter in section IV and V, we conclude in section VI.

II. NMSSM

NMSSM is a singlet extension of MSSM [1], which can solve the μ problem of MSSM. In this singlet extension of MSSM the superpotential can be written as [3],

$$\mathcal{W} = \lambda \hat{S} \hat{H}_u \cdot \hat{H}_d + \frac{\kappa}{3} \hat{S}^3 + h_u \hat{Q} \cdot \hat{H}_u \hat{U}_R^c + h_d \hat{H}_d \cdot \hat{Q} \hat{D}_R^c + h_e \hat{H}_d \cdot \hat{L} \hat{E}_R^c \quad (1)$$

where λ , κ , h_u , h_d and h_e are the dimensionless Yukawa couplings. In eq.(1), SU(2) doublets are

$$\hat{Q} = \begin{pmatrix} \hat{U}_L \\ \hat{D}_L \end{pmatrix}, \hat{L} = \begin{pmatrix} \hat{\nu}_L \\ \hat{E}_L \end{pmatrix}, \hat{H}_u = \begin{pmatrix} \hat{H}_u^+ \\ \hat{H}_u^0 \end{pmatrix}, \hat{H}_d = \begin{pmatrix} \hat{H}_d^0 \\ \hat{H}_d^- \end{pmatrix}$$

soft SUSY breaking terms, which correspond to the masses and couplings of fields, mentioned in eq.(1), are

$$\begin{aligned} -\mathcal{L}_{soft} = & m_{H_u}^2 |H_u|^2 + m_{H_d}^2 |H_d|^2 + m_S^2 |S|^2 \\ & + m_Q^2 |Q|^2 + m_U^2 |U_R|^2 + m_D^2 |D_R|^2 + m_L^2 |L|^2 + m_E^2 |E_R|^2 \\ & + (\lambda A_\lambda H_u \cdot H_d S + \frac{1}{3} \kappa A_\kappa S^3 + B_\mu H_u \cdot H_d \\ & + h_u A_u Q \cdot H_u U_R^c - h_d A_d Q \cdot H_d D_R^c - h_e A_e L \cdot H_d E_R^c + h.c.) \end{aligned} \quad (2)$$

Higgs potential can be obtained from the F, D and soft SUSY breaking terms and it is given as,

$$\begin{aligned} V = & |\lambda(H_u^+ H_d^- - H_u^0 H_d^0) + \kappa S^2|^2 \\ & + (m_{H_u}^2 + |\mu + \lambda S|^2)(|H_u^0|^2 + |H_u^+|^2) + (m_{H_d}^2 + |\mu + \lambda S|^2)(|H_d^0|^2 + |H_d^-|^2) \\ & + \frac{g_1^2 + g_2^2}{8} (|H_u^0|^2 + |H_u^+|^2 - |H_d^0|^2 - |H_d^-|^2)^2 + \frac{g_2^2}{2} |H_u^+ H_d^{0*} + H_u^0 H_d^{-*}|^2 \\ & + m_S^2 |S|^2 + (\lambda A_\lambda (H_u^+ H_d^- - H_u^0 H_d^0) S + \frac{1}{3} \kappa A_\kappa S^3 + B\mu (H_u^+ H_d^- - H_u^0 H_d^0) \\ & + h.c.) \end{aligned} \quad (4)$$

Here g_1 and g_2 represent $U(1)_Y$ and $SU(2)$ couplings respectively. After expanding Higgs potential around the real natural vevs v_u , v_d and s , considering minimization conditions, Higgs mass matrices can be found, see [3] for more discussion.

The neutralino mass matrix of NMSSM in the basis $(\tilde{B}, \tilde{W}^0, \tilde{H}_d^0, \tilde{H}_u^0, \tilde{S})$ is given by,

$$\mathcal{M}_\chi = \begin{pmatrix} M_1 & 0 & \frac{-g_1 v_d}{\sqrt{2}} & \frac{g_1 v_u}{\sqrt{2}} & 0 \\ 0 & M_2 & \frac{g_2 v_d}{\sqrt{2}} & \frac{-g_2 v_u}{\sqrt{2}} & 0 \\ \frac{-g_1 v_d}{\sqrt{2}} & \frac{g_2 v_d}{\sqrt{2}} & 0 & -\mu_{eff} & -\lambda v_u \\ \frac{g_1 v_u}{\sqrt{2}} & \frac{-g_2 v_u}{\sqrt{2}} & -\mu_{eff} & 0 & -\lambda v_d \\ 0 & 0 & -\lambda v_u & -\lambda v_d & 2\kappa s \end{pmatrix} \quad (6)$$

R parity conservation in the scale invariant version of NMSSM puts LSP as a natural candidate of dark matter. Neutralino, as a linear combination of neutral components of superpartners, see eq.(7), plays the role of LSP in most of the cases.

$$|\tilde{\chi}_1^0\rangle = N_{11}|\tilde{B}\rangle + N_{12}|\tilde{W}^0\rangle + N_{13}|\tilde{H}_d^0\rangle + N_{14}|\tilde{H}_u^0\rangle + N_{15}|\tilde{S}\rangle \quad (7)$$

In the neutralino, bino, wino, higgsinos and singlino-fractions are $N_{11}^2, N_{12}^2, N_{13}^2 + N_{14}^2$ and N_{15}^2 respectively. Using micrOMEGAs 3.1 code [35] we find a bench mark point with

Parameters	BM Point
N_{11}, N_{15}	0.989, -0.039
N_{12}, N_{13}, N_{14}	0.055, -0.123, 0.035
$\sigma_{SI}^p \times 10^{-10}$ pb	5.8
$\sigma_{SD}^p \times 10^{-6}$ pb	6.2
$\sigma_{SI}^n \times 10^{-10}$ pb	5.9
$\sigma_{SD}^n \times 10^{-6}$ pb	5.4

TABLE I. The fractions of bino, wino, higgsinos and singlino in neutralino correspond to bench mark point of Table-(III). The values of spin-independent and spin dependent cross-sections correspond to proton and neutron also shown, which is lying outside the current limit of XENON100 [14] and can be tested in XENON1T [45]

parameters as shown in Table-(III). This set of parameters give a SUSY spectrum (Table-III), containing a 130 GeV bino dark matter with gauginos fractions shown in Table-(I). It also contains a ~ 125 GeV CP even Higgs as the lightest Higgs along with a light pseudo

scalar Higgs of mass ~ 68 GeV. Due to its singlet nature, this pseudo scalar Higgs can escape the lower bound of LEP [46]. The total decay width of Higgs and its branching ratios have also calculated using micrOMEGAs package. We mentioned the decay channels and branching ratios of lightest CP even Higgs in Table-(II) and compared them with their Standard Model counterparts. The micrOMEGAs 3.1 code [35] was also used to calculate

Decay Processes	Branching Ratios (NMSSM)	$R = \frac{BR(H_i \rightarrow XX)}{BR(H_{SM} \rightarrow XX)}$
$H \rightarrow b\bar{b}$	6.57×10^{-1}	1.10
$H \rightarrow WW$	1.77×10^{-1}	≈ 0.90
$H \rightarrow ZZ$	2.072×10^{-2}	≈ 0.99
$H \rightarrow \gamma\gamma$	1.61×10^{-3}	≈ 0.69
Γ_{total}	4.479×10^{-3}	$\frac{\Gamma_{total}^i}{\Gamma_{total}^{SM}} = 1.13$

TABLE II. Branching ratios in different channels and total decay width for NMSSM parameter space. R gives the comparison of these Branching ratios to their SM values.

the relic density of our bino dark matter and as it can be seen from Table-(III) that the value of relic density agrees with the WMAP-PLANCK [12, 13] results i.e $\Omega_\chi h^2 = 0.1199 \pm 0.0027$.

III. GAMMA RAY SIGNAL AND INTERNAL BREMSSTRAHLUNG

Recently, 130 GeV gamma ray signal coming from the vicinity of Galactic Center, has been observed in Fermi-LAT experiment [47] and it was found that a dark matter with mass 129 ± 2.4 GeV [18] and cross-section $\langle\sigma v\rangle_{\gamma\gamma} = (1.27 \pm 0.32) \times 10^{-27} \text{cm}^3 \text{sec}^{-1}$ [18–26] fits the signal very well. The wino or higgsino dark matter can satisfy these limits, but as suggested by [29], they will be ruled out by continuum constraints. A bino dark matter with internal bremsstrahlung can explain the observed feature of Fermi-LAT experiment [47] and at the same time avoids continuum constraints. This idea will be discussed now in detail.

We take the scenario of Fig.(1), where dark matter annihilates into two fermions. In this case, s-wave annihilation cross section will be helicity suppressed and p-wave contribution will be velocity suppressed [48]. The presence of photon in the final state can lift the

Parameters at EW scale		Mass Spectrum	
$\tan\beta$	1.65	SM-like Higgs Boson	
μ_{eff}	-208	M_{H_1} [GeV]	125.32
λ	-0.62	Remaining Higgs spectrum	
κ	-0.16	M_{H_2} [GeV]	150.68
A_λ [GeV]	-380	M_{H_3} [GeV]	453.09
A_κ [GeV]	-40	M_{A_1} [GeV]	67.47
$M_{\tilde{L}_2}$ [GeV]	152	M_{A_2} [GeV]	453.52
$M_{\tilde{\mu}_R}$ [GeV]	152	M_{H^\pm} [GeV]	444.21
$M_{\tilde{L}_3}$ [GeV]	180	Sparticle masses and stop mixing	
$M_{\tilde{\tau}_R}$ [GeV]	180	$m_{\tilde{g}}$ [GeV]	1352.6
M_1 [GeV]	129	$m_{\tilde{\chi}_1^\pm}$ [GeV]	216.8
M_2 [GeV]	260	$m_{\tilde{\chi}_2^\pm}$ [GeV]	284.2
M_3 [GeV]	1300	$m_{\tilde{\chi}_1^0}$ [GeV]	130.1
		$m_{\tilde{\chi}_2^0}$ [GeV]	134.6
		$m_{\tilde{\chi}_3^0}$ [GeV]	233.5
		$m_{\tilde{\chi}_4^0}$ [GeV]	235.6
		$m_{\tilde{\chi}_5^0}$ [GeV]	285.7
		Relic Density	
		Ωh^2	0.107

TABLE III. The values of the parameters specified at electroweak scale and the output spectrum of SUSY particles.

helicity suppression of $(m_f/m_\chi)^2$ in the s wave annihilation cross-section, but suppress it by α_{em} [31, 49]. In Fig.(1), three possibilities have been shown, the first one correspond to virtual internal bremsstrahlung (VIB) and the last two correspond to final state radiation (FSR), jointly known as internal bremsstrahlung (IB). The enhanced annihilation cross-section can be obtained through internal bremsstrahlung when the mass of neutralino is nearly degenerate with slepton mass and massless leptons are present in final state. The

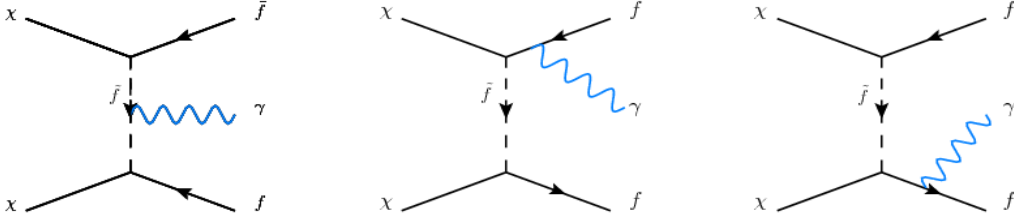


FIG. 1. Dark Matter annihilation into two fermion, first figure corresponds to virtual internal bremsstrahlung (VIB) and the other two correspond to Final state radiation (FSR), jointly known as internal bremsstrahlung

annihilation cross-section for the process $\chi\chi \rightarrow \bar{f}f\gamma$, where γ is a virtual photon is given by [39, 48, 50],

$$\begin{aligned} \langle\sigma v\rangle_{v\rightarrow 0} = \frac{\alpha_{em}|\tilde{g}_R|^4}{64\pi^2 m_\chi^2} & \left\{ \frac{3+4\mu_R}{1+\mu_R} + \frac{4\mu_R^2-3\mu_R-1}{2\mu_R} \log \frac{\mu_R-1}{\mu_R+1} \right. \\ & \left. + (1+\mu_R) \left[\frac{\pi^2}{6} - \left(\log \frac{\mu_R+1}{2\mu_R} \right)^2 - 2\text{Li}_2 \left(\frac{\mu_R+1}{2\mu_R} \right) \right] \right\} + (R \leftrightarrow L) \end{aligned} \quad (8)$$

where $\text{Li}_2(z) = \sum_{k=1}^{\infty} z^k/k^2$, $\mu_{R,L} \equiv m_{\tilde{f}_{R,L}}^2/m_\chi^2$ and $\tilde{g}_R(\tilde{g}_L)$ is the coupling between neutralino, leptons and sleptons. This expression is valid for the massless fermions in the final state, within MSSM scenario. We used micrOMEGAs3.1 [35] code for our dark matter calculations and found that bino is the possible dark matter for our bench mark point, see Table-(I). Since bino is the dark matter candidate, we can use the same annihilation cross-section of eq.(8), for our calculation. The Yukawa couplings in MSSM scenario, can be defined as [51].

$$\tilde{g}_L = -\frac{2Q_f \mp 1}{\sqrt{2}} g_2 \tan\theta_W N_{11} \mp \frac{g_2}{\sqrt{2}} N_{12} \quad (9)$$

$$\tilde{g}_R = \sqrt{2}Q_f g_2 \tan\theta_W N_{11} \quad (10)$$

where g_2 is the $SU(2)$ coupling and θ_W is the Weinberg angle. N_{11} and N_{12} has defined in eq.(7) and their values have given in Table.(I). In eq.(9), \mp signs correspond to isospin, $T_3 = \pm \frac{1}{2}$ respectively. In our bench mark scenario, the values of the couplings as given by eq.(9, 10) are,

$$\tilde{g}_L \approx 0.27, \quad \tilde{g}_R \approx -0.50 \quad (11)$$

After using these values with corresponding N_{11} and N_{12} from Table.(I), annihilation cross-section for electron-positron final state comes,

$$\langle\sigma v\rangle \approx 2.4 \times 10^{-29} \text{cm}^3/\text{sec} \quad (12)$$

which is less than the required cross-section ($O \sim 10^{-27}$ [18]), for fitting the signal of 130 GeV dark matter and we need a boost factor of ~ 590 to explain Fermi-LAT data [47].

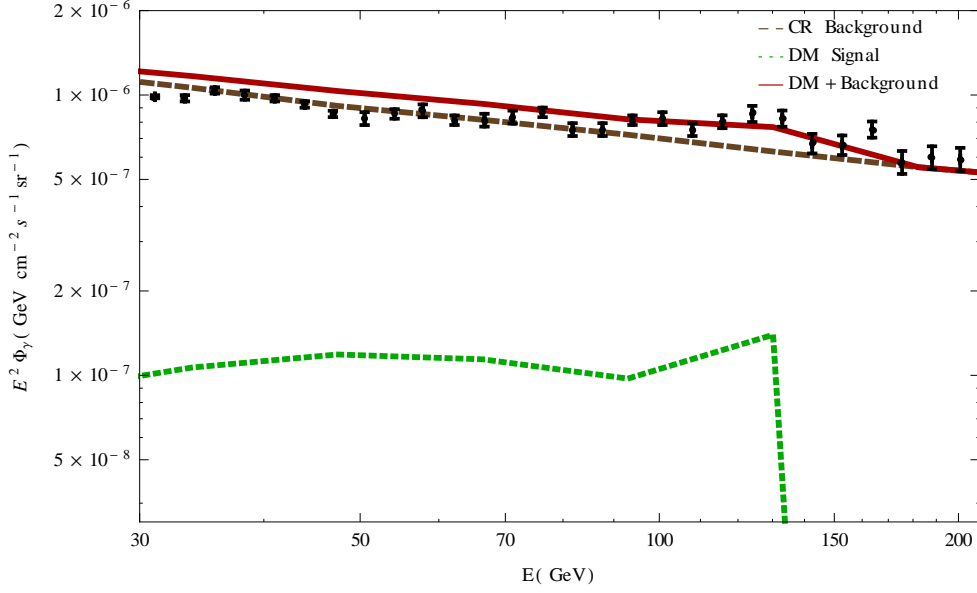


FIG. 2. Diffuse γ -ray flux for 130 GeV, bino dark matter in the bench mark scenario of Table-(III). FERMI-LAT data [47] has been shown for comparison.

IV. INDIRECT DETECTION

Indirect detection of dark matter relies on the observations of its annihilation products. There are various experiments like IceCube [52], PAMELA [53] and Fermi-LAT [47], which are looking for the different form of annihilation products of dark matter. Recently, AMS-02 experiment [54] observed an excess in positron flux, which may be the indirect signal of dark matter, but to satisfy AMS-02 data, one needs a \sim TeV range dark matter, which is not the case for our bench mark point. Hence in this work, we do not attempt to fit the positron excess observed in AMS-02 experiment [54]. In section-III, we discussed the effect of internal bremsstrahlung on the dark matter annihilation cross-section, since dark matter is a majorana particle, its cross section for the process of eq.(13), will be suppressed by helicity conservation.

$$\chi\chi \rightarrow f\bar{f}\gamma \quad (13)$$

If there is a photon present in the final state, as shown in Fig.(1), helicity suppression can

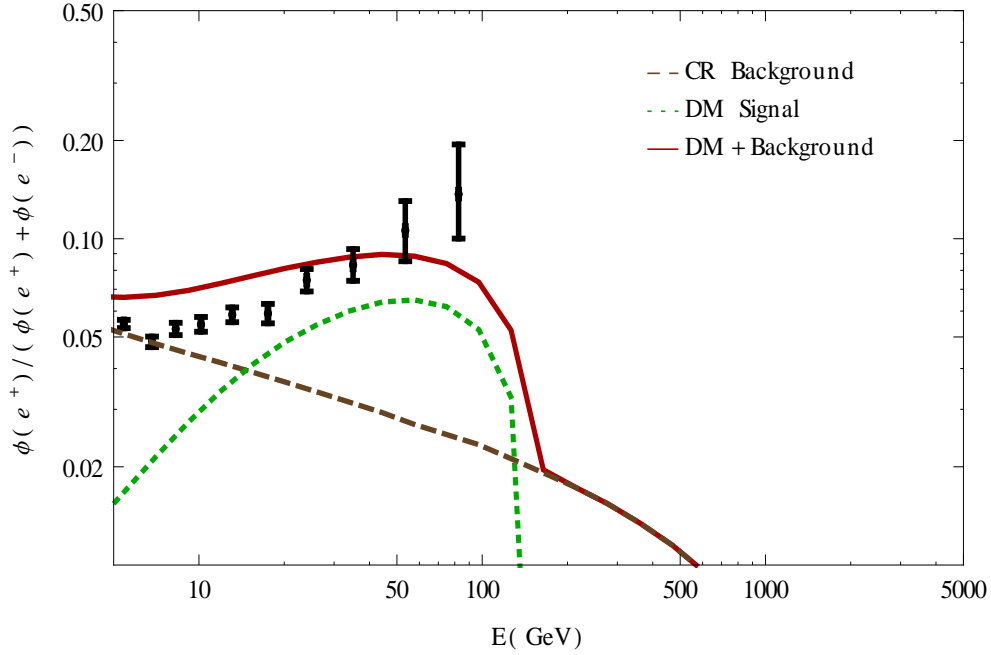


FIG. 3. Ratio of the positron flux $\phi(e^+)$ to the total flux $(\phi(e^+) + \phi(e^-))$ vs Energy for 130 GeV, bino dark matter in the bench mark scenario of Table.(III). Background and dark matter signals with PAMELA data [53] have been shown for comparison.

be avoided, leaving behind α_{em} suppression, which gives a much larger cross-section. We got photon flux from micrOMEGAs 3.1 code [35] for our bench mark scenario and used this flux with boosted (~ 590) annihilation cross section in GALPROP code [36, 37]. In Fig.(2), GALPROP output for diffuse gamma ray flux using isothermal density profile [38] has been plotted as a function of energy. It can be seen from Fig.(2) that there is a clear bump at 130 GeV, which satisfy the observed feature of Fermi-LAT data [47]. Since, a boost factor of ~ 590 is required to explain Fermi-LAT data [47], we explored the effects of this boost factor on the positron, electron and antiproton flux, that we will discuss now in details.

PAMELA satellite [53], which detects antimatter, has observed an excess in the differential ratio $\frac{\phi(e^+)}{\phi(e^+ + e^-)}$, which seems to indicate the presence of dark matter annihilation products. As in the case of gamma, we use the electron, positron and antiproton fluxes obtained from micrOMEGAs, in the GALPROP [36, 37] with a boosted annihilation cross-section as before. The output spectrum of positron obtained from GALPROP, relative to electron for 130 GeV bino dark matter has been plotted in Fig.(3). We have also plotted PAMELA data for comparison and found that boost factor of ~ 590 agrees with the positron excess

observed in PAMELA data [53]. PAMELA data can be explained with a large boost factor that has been discussed in detail [39, 40], where authors suggest, the presence of massive black hole as a reason for the large boost factor. In [39], flux ratio has been plotted for different mass range of dark matter and suggested that neutralino with mass greater than 100 GeV can fit the signal well, but the shape of the signal gets flatter with increasing mass of dark matter. This is the case for our bench mark point, which satisfying Fermi-LAT data under the constraint of PAMELA experiment. The low energy region of the plot in Fig.(3), seems to be in disagreement with the observed data, but due to solar modulation effect, the constraint of PAMELA experiment in this region is relaxed.

In addition we also do not see any excess in the $(\phi(e^+) + \phi(e^-))$ flux observed by Fermi-LAT [41, 42] experiment, as shown in Fig.(4). And similarly no excess is observed in the case of antiproton flux observed by PAMELA [43, 44] as shown in Fig.(5).

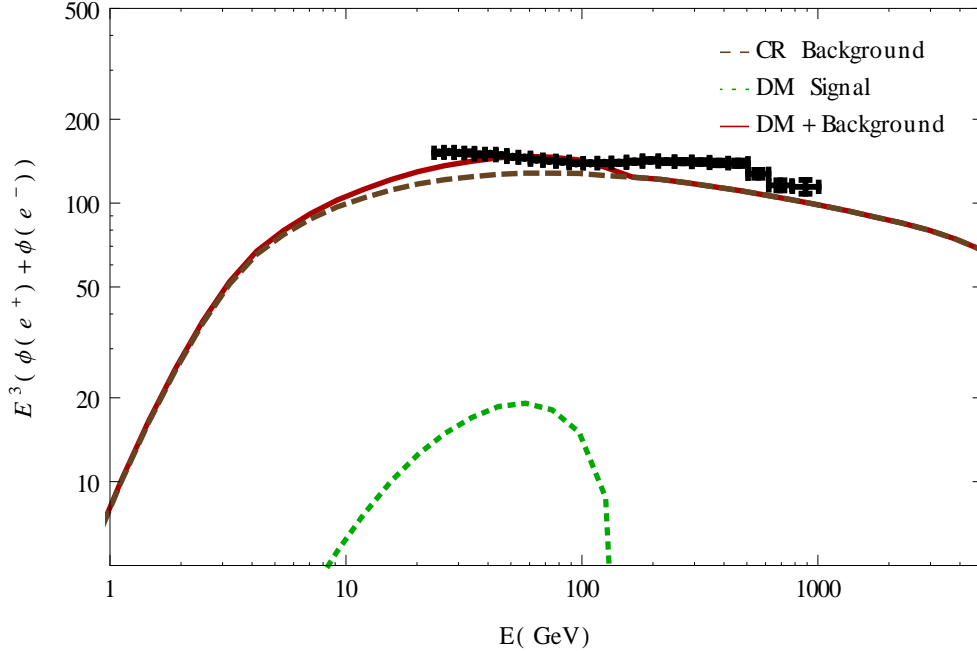


FIG. 4. The $(\phi(e^+) + \phi(e^-))$ flux for 130 GeV bino dark matter, Fermi-LAT data [41, 42] has been shown for comparison. Green dotted line denotes the dark matter signal and Brown dashed line denotes the background

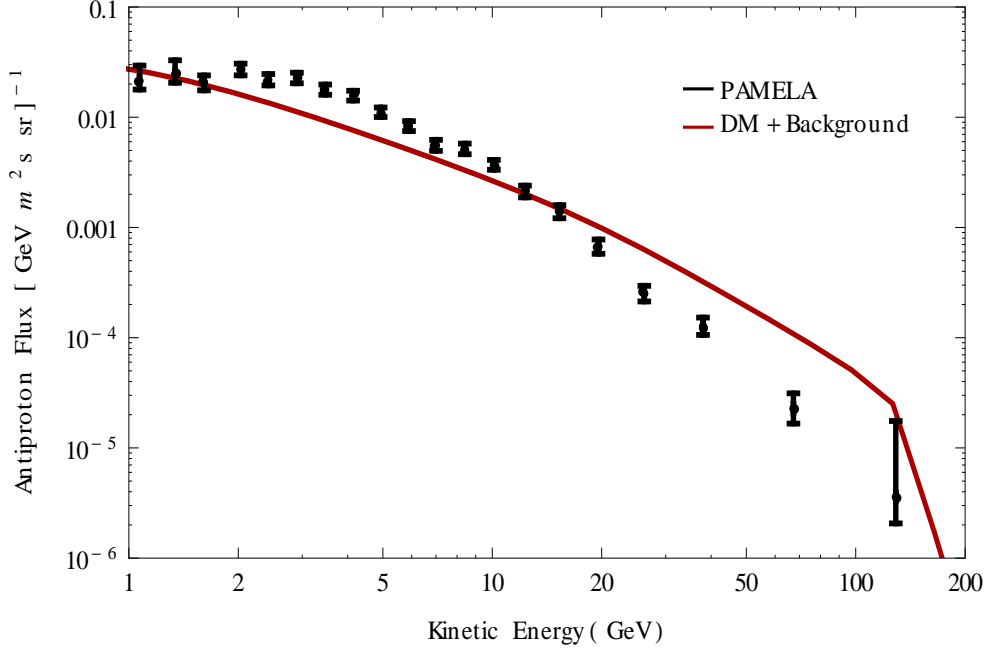


FIG. 5. The $(e^+ + e^-)$ flux for 130 GeV bino dark matter, Fermi-LAT data [41, 42] has been shown for comparison. Green dotted line denotes the dark matter signal and Brown dashed line denotes the background

V. DIRECT DETECTION

In the direct detection of Weakly Interacting Massive Particle (WIMP), elastic scattering cross-section of WIMP from a heavy nuclei like Xenon or Germanium, plays an important role. There are possibilities for different types of interactions (Fig.6) between WIMP and matter nuclei, but two of them play the major role. Spin-spin interaction is one of the important interaction, where WIMP couples to the spin of the nucleus. The other important coherent interaction is scalar interaction, in which WIMP couples to the mass of the nucleus. The low energy effective Lagrangian for these two interactions is [55],

$$\mathcal{L}_{eff} = c_q \bar{\chi} \chi \bar{q} q + d_q \bar{\chi} \gamma^\mu \gamma_5 \chi \bar{q} \gamma_\mu \gamma_5 q \quad (14)$$

where c_q and d_q are the couplings corresponding to spin independent and dependent interactions respectively. As pointed out in [34], these couplings are model dependent and in NMSSM, c_q will be proportional to the coupling of neutralino-neutralino to Higgs. Since in our case squarks are heavy (\sim TeV), so they decouple easily and don't play any significant role in the scattering processes.

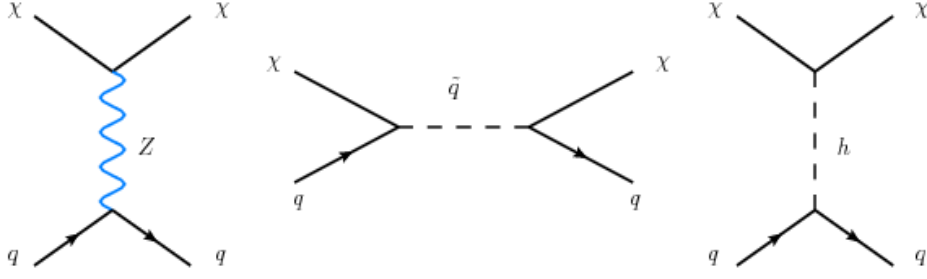


FIG. 6. Feynman diagrams for spin dependent and independent elastic scattering of neutralino from quarks.

We use micrOMEGAs 3.1 code [35], for the calculation of spin dependent and indepen-

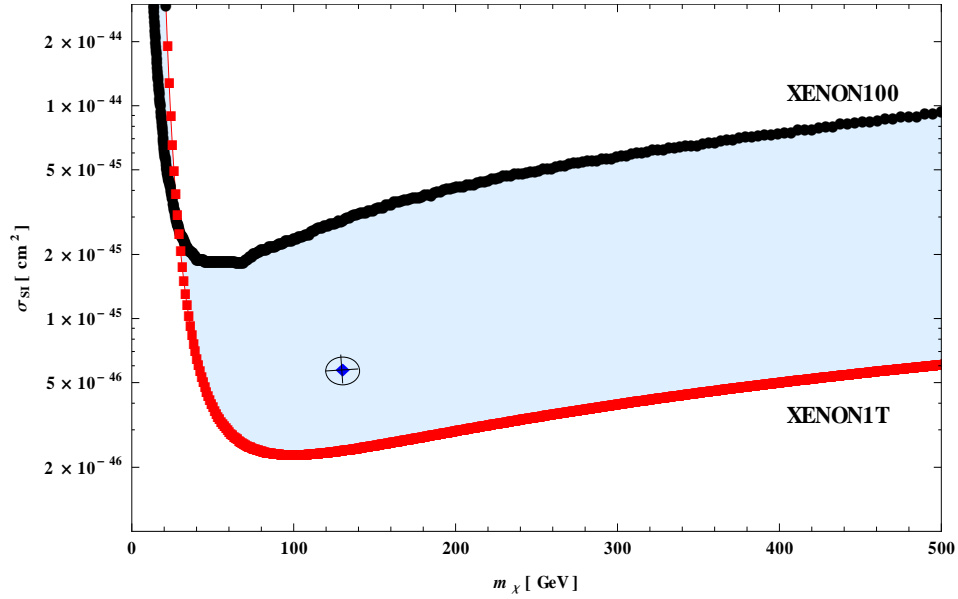


FIG. 7. Plot of spin independent cross-section versus neutralino mass. XENON100 [14] and XENON1T [45] data has shown for comparison.

dent cross-section for our bench mark scenario. We find scalar interaction cross-section, $\sigma_{SI}^p = 5.8 \times 10^{-10}$ pb for ~ 130 GeV neutralino. This cross-section goes beyond the current limit of XENON100 experiment, which is $\sigma_{SI}^p \sim 3 \times 10^{-9}$ pb for 130 GeV neutralino [14]. In Fig.(7), We plot σ_{SI}^p as a function of m_χ along with the exclusion limit from XENON100 [14] and XENON1T [45] experiments. It is clear that our point evades the current constraint of XENON100 and can be tested in XENON1T experiment.

Spin dependent interaction is mediated by Z boson and for scale invariant NMSSM, it can

be given as [34],

$$\sigma_{\text{SD}}^p \approx 4.0 \times 10^{-4} \text{pb} \left(\frac{|N_{13}|^2 - |N_{14}|^2}{0.1} \right)^2 \quad (15)$$

In our case, bino is the LSP and N_{13} , N_{14} components are very small, so it is easy to evade present bounds on spin dependent cross-section coming from Super-Kamiokande and IceCube experiments [52, 56], which is $\sim 2.7 \times 10^{-4} \text{pb}$ for $\sim 100 \text{ GeV}$ neutralino. Our result of $\sigma_{\text{SD}}^p = 6.21 \times 10^{-6} \text{pb}$ for $m_{\chi^0} \sim 130 \text{ GeV}$ is close to the value coming from analytical expression of eq.(15) and evades the present bounds. All the values of bino, wino, higgsino and singlino fractions with spin dependent and independent cross-sections are shown in Table-(I). This result can be further tested in future experiments [45, 57].

VI. CONCLUSION

In this paper, we explored the internal bremsstrahlung in the singlet extension of MSSM and found that it can give an explanation for recently observed feature in Fermi-LAT data. We discussed the internal bremsstrahlung in the NMSSM and fit the Fermi-LAT data for isothermal profile of dark matter. We have chosen light sleptons such as they lie near to the mass of dark matter to get an enhanced cross-section. In the internal bremsstrahlung case, to satisfy Fermi-LAT data, we need a boost factor of ~ 590 . The effect of the boost factor on the flux of electrons, positrons and antiprotons have been discussed in details and we do not observe any excess in the spectrum of electrons, positrons and antiprotons, over the CR background, as shown in Fig.(3,4,5). We also discussed the direct and indirect detection consequence of our dark matter scenario. It is clear from Fig.(7) that for spin independent cross-section, our bench mark point evades the current bound of XENON100 easily and can be tested in future experiments. Spin dependent cross-section also evades the present experimental bound and can be verified in future experiments.

[1] A. Djouadi, *Phys.Rept.* **459**, 1 (2008), [arXiv:hep-ph/0503173 \[hep-ph\]](#)

[2] M. DREES, *International Journal of Modern Physics A* **04**, 3635 (1989)

- [3] U. Ellwanger, C. Hugonie, and A. M. Teixeira, *Phys.Rept.* **496**, 1 (2010), [arXiv:0910.1785 \[hep-ph\]](#)
- [4] G. G. Ross and K. Schmidt-Hoberg, *Nucl.Phys.* **B862**, 710 (2012), [arXiv:1108.1284 \[hep-ph\]](#)
- [5] L. J. Hall, D. Pinner, and J. T. Ruderman, *JHEP* **1204**, 131 (2012), [arXiv:1112.2703 \[hep-ph\]](#)
- [6] S. King, M. Muhlleitner, and R. Nevzorov, *Nucl.Phys.* **B860**, 207 (2012), [arXiv:1201.2671 \[hep-ph\]](#)
- [7] Z. Kang, J. Li, and T. Li, *JHEP* **1211**, 024 (2012), [arXiv:1201.5305 \[hep-ph\]](#)
- [8] J.-J. Cao, Z.-X. Heng, J. M. Yang, Y.-M. Zhang, and J.-Y. Zhu, *JHEP* **1203**, 086 (2012), [arXiv:1202.5821 \[hep-ph\]](#)
- [9] D. A. Vasquez, G. Belanger, C. Boehm, J. Da Silva, P. Richardson, *et al.*, *Phys.Rev.* **D86**, 035023 (2012), [arXiv:1203.3446 \[hep-ph\]](#)
- [10] G. Aad *et al.* (ATLAS Collaboration), *Phys.Lett.* **B716**, 1 (2012), [arXiv:1207.7214 \[hep-ex\]](#)
- [11] S. Chatrchyan *et al.* (CMS Collaboration), *Phys.Lett.* **B716**, 30 (2012), [arXiv:1207.7235 \[hep-ex\]](#)
- [12] P. Ade *et al.* (Planck Collaboration)(2013), [arXiv:1303.5076 \[astro-ph.CO\]](#)
- [13] G. Hinshaw *et al.* (WMAP Collaboration)(2012), [arXiv:1212.5226 \[astro-ph.CO\]](#)
- [14] E. Aprile *et al.* (XENON100 Collaboration), *Phys.Rev.Lett.* **109**, 181301 (2012), [arXiv:1207.5988 \[astro-ph.CO\]](#)
- [15] Z. Ahmed *et al.* (CDMS-II Collaboration), *Science* **327**, 1619 (2010), [arXiv:0912.3592 \[astro-ph.CO\]](#)
- [16] Z. Ahmed *et al.* (CDMS-II Collaboration), *Phys.Rev.Lett.* **106**, 131302 (2011), [arXiv:1011.2482 \[astro-ph.CO\]](#)
- [17] W. Atwood *et al.* (LAT Collaboration), *Astrophys.J.* **697**, 1071 (2009), [arXiv:0902.1089 \[astro-ph.IM\]](#)
- [18] C. Weniger, *JCAP* **1208**, 007 (2012), [arXiv:1204.2797 \[hep-ph\]](#)
- [19] E. Tempel, A. Hektor, and M. Raidal, *JCAP* **1209**, 032 (2012), [arXiv:1205.1045 \[hep-ph\]](#)
- [20] A. Hektor, M. Raidal, and E. Tempel, *Astrophys.J.* **762**, L22 (2013), [arXiv:1207.4466 \[astro-ph.HE\]](#)
- [21] M. Su and D. P. Finkbeiner(2012), [arXiv:1206.1616 \[astro-ph.HE\]](#)
- [22] M. Su and D. P. Finkbeiner(2012), [arXiv:1207.7060 \[astro-ph.HE\]](#)
- [23] D. Hooper and T. Linden, *Phys.Rev.* **D86**, 083532 (2012), [arXiv:1208.0828 \[astro-ph.HE\]](#)

- [24] A. Hektor, M. Raidal, and E. Tempel(2012), [arXiv:1208.1996 \[astro-ph.HE\]](#)
- [25] N. Mirabal, Mon.Not.Roy.Astron.Soc. **429**, L109 (2013), [arXiv:1208.1693 \[astro-ph.HE\]](#)
- [26] H.-S. Zechlin and D. Horns, [JCAP **1211**, 050 \(2012\)](#), [arXiv:1210.3852 \[astro-ph.HE\]](#)
- [27] D. Whiteson, [JCAP **1211**, 008 \(2012\)](#), [arXiv:1208.3677 \[astro-ph.HE\]](#)
- [28] A. Hektor, M. Raidal, and E. Tempel(2012), [arXiv:1209.4548 \[astro-ph.HE\]](#)
- [29] T. Cohen, M. Lisanti, T. R. Slatyer, and J. G. Wacker, [JHEP **1210**, 134 \(2012\)](#), [arXiv:1207.0800 \[hep-ph\]](#)
- [30] B. Shakya(2012), [arXiv:1209.2427 \[hep-ph\]](#)
- [31] L. Bergstrom, [Phys.Lett. **B225**, 372 \(1989\)](#)
- [32] L. Bergstrom, T. Bringmann, M. Eriksson, and M. Gustafsson, [Phys.Rev.Lett. **95**, 241301 \(2005\)](#), [arXiv:hep-ph/0507229 \[hep-ph\]](#)
- [33] D. Das, U. Ellwanger, and P. Mitropoulos, [JCAP **1208**, 003 \(2012\)](#), [arXiv:1206.2639 \[hep-ph\]](#)
- [34] G. Chalons, M. J. Dolan, and C. McCabe, [JCAP **1302**, 016 \(2013\)](#), [arXiv:1211.5154 \[hep-ph\]](#)
- [35] G. Belanger, F. Boudjema, A. Pukhov, and A. Semenov(2013), [arXiv:1305.0237 \[hep-ph\]](#)
- [36] A. W. Strong, I. V. Moskalenko, and V. S. Ptuskin, [Ann.Rev.Nucl.Part.Sci. **57**, 285 \(2007\)](#), [arXiv:astro-ph/0701517 \[astro-ph\]](#)
- [37] I. Moskalenko and A. Strong, [Astrophys.J. **493**, 694 \(1998\)](#), [arXiv:astro-ph/9710124 \[astro-ph\]](#)
- [38] J. N. Bahcall and R. Soneira, [Astrophys.J.Suppl. **44**, 73 \(1980\)](#)
- [39] L. Bergstrom, T. Bringmann, and J. Edsjo, [Phys.Rev. **D78**, 103520 \(2008\)](#), [arXiv:0808.3725 \[astro-ph\]](#)
- [40] S. Mohanty, S. Rao, and D. Roy, [JHEP **1211**, 175 \(2012\)](#), [arXiv:1208.0894 \[hep-ph\]](#)
- [41] A. A. Abdo *et al.* (Fermi LAT Collaboration), [Phys.Rev.Lett. **102**, 181101 \(2009\)](#), [arXiv:0905.0025 \[astro-ph.HE\]](#)
- [42] M. Ackermann *et al.* (Fermi LAT Collaboration), [Phys.Rev. **D82**, 092004 \(2010\)](#), [arXiv:1008.3999 \[astro-ph.HE\]](#)
- [43] O. Adriani, G. Barbarino, G. Bazilevskaya, R. Bellotti, M. Boezio, *et al.*, [Phys.Rev.Lett. **102**, 051101 \(2009\)](#), [arXiv:0810.4994 \[astro-ph\]](#)
- [44] O. Adriani *et al.* (PAMELA Collaboration), [Phys.Rev.Lett. **105**, 121101 \(2010\)](#), [arXiv:1007.0821 \[astro-ph.HE\]](#)
- [45] E. Aprile (XENON1T collaboration)(2012), [arXiv:1206.6288 \[astro-ph.IM\]](#)

- [46] S. Schael *et al.* (ALEPH Collaboration, DELPHI Collaboration, L3 Collaboration, OPAL Collaboration, LEP Working Group for Higgs Boson Searches), [Eur.Phys.J. C47](#), 547 (2006), [arXiv:hep-ex/0602042 \[hep-ex\]](#)
- [47] M. Ackermann *et al.* (Fermi LAT Collaboration), [Phys.Rev.Lett. 108](#), 011103 (2012), [arXiv:1109.0521 \[astro-ph.HE\]](#)
- [48] T. Bringmann, X. Huang, A. Ibarra, S. Vogl, and C. Weniger, [JCAP 1207](#), 054 (2012), [arXiv:1203.1312 \[hep-ph\]](#)
- [49] R. Flores, K. A. Olive, and S. Rudaz, [Phys.Lett. B232](#), 377 (1989)
- [50] N. F. Bell, J. B. Dent, A. J. Galea, T. D. Jacques, L. M. Krauss, *et al.*, [Phys.Lett. B706](#), 6 (2011), [arXiv:1104.3823 \[hep-ph\]](#)
- [51] H. E. Haber and G. L. Kane, [Phys.Rept. 117](#), 75 (1985)
- [52] R. Abbasi *et al.* (IceCube Collaboration), [Phys.Rev. D85](#), 042002 (2012), [arXiv:1112.1840 \[astro-ph.HE\]](#)
- [53] O. Adriani *et al.* (PAMELA Collaboration), [Nature 458](#), 607 (2009), [arXiv:0810.4995 \[astro-ph\]](#)
- [54] M. Aguilar *et al.* (AMS Collaboration), [Phys.Rev.Lett. 110](#), 141102 (2013)
- [55] G. Jungman, M. Kamionkowski, and K. Griest, [Phys.Rept. 267](#), 195 (1996), [arXiv:hep-ph/9506380 \[hep-ph\]](#)
- [56] T. Tanaka *et al.* (Super-Kamiokande Collaboration), [Astrophys.J. 742](#), 78 (2011), [arXiv:1108.3384 \[astro-ph.HE\]](#)
- [57] S. Fiorucci (LUX Collaboration)(2013), [arXiv:1301.6942 \[astro-ph.IM\]](#)